




Original Article

Structure and seismo-tectonic investigation of the Sarıgöl- Buldan region, Western Anatolia, by using gravity and seismicity data

ALTINOĞLU Fatma Figen ^{1*}  <https://orcid.org/0000-0001-6261-5658>;  e-mail: faltinoglu@pau.edu.tr

POLAT Gulten²  <https://orcid.org/0000-0002-6956-7385>; e-mail: gulten.polat@yeditepe.edu.tr

* Corresponding author

¹ Department of Geological Engineering, Faculty of Engineering, Pamukkale University, Denizli 20017, Turkey

² Department of Civil Engineering, Yeditepe University, 26 Ağustos Yerleşkesi, Kağıtsdağı Cad 34755, Istanbul, Turkey

Citation: Altinoğlu FF, Polat G (2022) Structure and seismo-tectonic investigation of the Sarıgöl- Buldan region, Western Anatolia, by using gravity and seismicity data. Journal of Mountain Science 19(10). <https://doi.org/10.1007/s11629-022-7452-0>

© Science Press, Institute of Mountain Hazards and Environment, CAS and Springer-Verlag GmbH Germany, part of Springer Nature 2022

Abstract: The parameter b (commonly referred to as the b -value) is one of the most significant seismic parameters to describe the seismicity of an investigated region. In this study, the structural framework of the Sarıgöl- Buldan region located in the intersection area of the western Anatolian graben system in Turkey was investigated by using seismicity and gravity data. As known, western Anatolia is one of the most seismically active regions of the Anatolian plate. Therefore, seismic activity in this region is very high. Analysis of the Bouguer gravity data enabled to define the shallow subsurface structure of the study area. Results from the gravity analysis indicated that the sediment basement depth varied from 0.1 km and 2.1 km. We also detected many NW-SE, E-W, and NE-SW trending lineaments that may be faults or fractures, and the NW-SE trending the Denizli basin lies to the east of the Alaşehir basin. We observed that the findings from this analysis seem compatible with the regional geological trend. In addition to this, the seismicity of the region was analyzed by using the frequency-magnitude distribution to find out the seismic hazard risk. The most useful way in the analysis of the seismic hazard studies is to reveal the location of the earthquake boundary, which produces devastating big seismic events because such studies

make it possible to forecast the location of possible future earthquakes and improve seismic hazard maps. The b -value for this study region was estimated by using the maximum likelihood method. Variations in the b -value were observed, which range from ≈ 0.2 to 2. A higher b -value was detected in the Buldan horst and surrounding area. In contrast to this, lower b -values were observed in the northeast part of the interaction region between the Denizli and the Alaşehir grabens. The positive Bouguer anomaly values as high as +10 mGal and low b -values in the north-eastern part of the study region were interpreted as indicating a thinner crustal root. In comparison, negative Bouguer anomaly values were observed in the Alaşehir and the Denizli grabens. Also, in these grabens, intermediate to high b -values were found. This suggests that there is a relation between gravity anomaly and b -value. This relation is strongly related to the normal faulting mechanism existing in the region.

Keywords: Bouguer; Gravity; Seismicity; Stress; b -value; the Sarıgöl- Buldan region

1 Introduction

The Anatolian Plate started to move in the westward direction (Papazachos 1999) as a result of

Received: 14-Apr-2022
1st Revision: 16-May-2022
2nd Revision: 19-Jul-2022
Accepted: 16-Aug-2022

the collision between the Eurasian and Arabian Plates in the Middle Miocene (Şengör et al. 1985). In addition to this, the African plate subduction beneath the Anatolian block resulted in developing the N-S directional extension in Western Anatolia (Şengör and Yılmaz 1981) (Fig. 1). A recent study of Meng et al. (2021) showed that the Aegean plate connected with the Western Anatolia extensional province on the Turkish mainland. The revealed extensional region continues with the Aegean subduction zone propagating southwards by up to 1000 km (Seward et al. 2009) due to slab rollback. The African slab retreats; it is pulling parts of the upper plate of Anatolia and the Aegean with it to the south, causing N-S extension (e.g., Mercier et al. 1989; Jolivet et al. 2013). The tectonic escape remarkably affects extensional tectonics in the western part of the Anatolian plate. Western Anatolia is known to be an area of widespread active continental extension (Bozkurt and Mittweide 2001). Tectonic and geologic processes of this region are significantly affected by subduction, the ongoing plate collision, and the transition between the upper plate into numerous smaller microplates (Meng et al. 2021). Therefore, the investigation of the complex tectonic structure of Western Anatolia has been an important issue of many studies in the literature (Seyitoğlu and Scott 1996; Koçyiğit et al. 1999; Yılmaz et al. 2000; Bozkurt 2003; Bozkurt and Sözbilir 2004; Kaymakçı 2006; Gessner et al. 2013). Previous geological studies (e.g., Seyitoğlu and Scott 1991; Seyitoğlu and Scott 1992a; Seyitoğlu and Scott 1992b; Hetzel et al. 1998) indicated that many graben-horst systems developed under this extensional regime.

In particular, the rollback process driven by the African plate

significantly influences the geometrically complex normal fault systems, and earlier transtensional systems. This retreating process significantly plays a role to form upper crustal extension and active seismicity in this area. Regional extensional basins, fault systems and sedimentary and volcanic deposits in the region may additionally indicate to be the results of the regime controlling the region.

Two-stage extensions in the Western Anatolia were suggested by Bozkurt (2001) and Bozkurt and Sözbilir (2004). According to these studies, the first stage was initiated in Late Oligocene-Early Miocene,

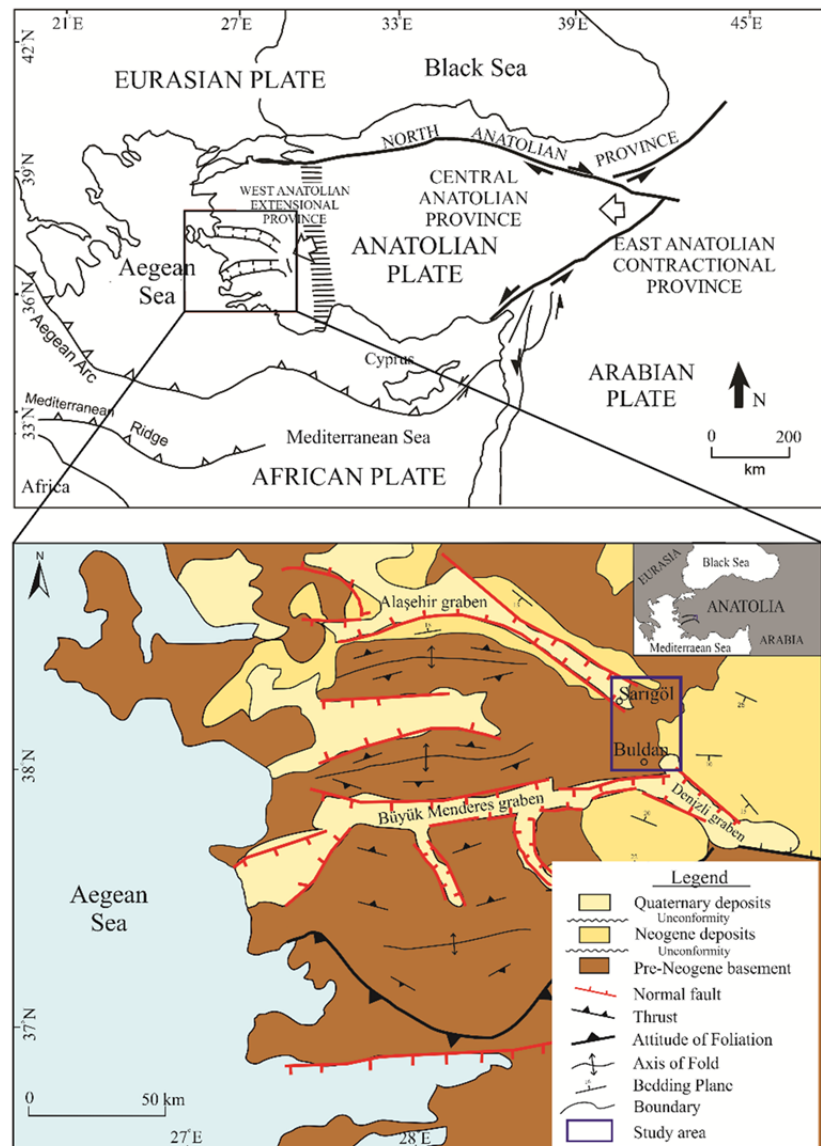


Fig. 1 Simplified tectonic map of Turkey showing major neotectonic structures (modified from Bozkurt & Sözbilir 2004) and the main tectonic settings of Western Anatolia modified from Konak and Şenel (2002). The location of the study area is shown with the blue rectangle.

and the second stage started in the Pliocene (~ 5 Ma) age (Bozkurt and Sözbilir 2004). The propounded tectonic models for the origin of extension in western Anatolia are (1) tectonic escape (Şengör et al. 1985; Şengör and Yılmaz 1981; Dewey and Şengör 1979; Şengör 1979), (2) back-arc extension (McKenzie 1978; Le Pichon and Angelier 1979, 1981; Meulenkamp et al. 1988; Spakman et al. 1988), and (3) orogenic collapse (Seyitoğlu and Scott 1996; Dilek and Whitney 2000). E-W trending the Büyük Menderes and the Alaşehir grabens and NW-SE trending the Denizli graben are the main tectonic structures of western Anatolia, and the basement rocks of the metamorphic Menderes massif are located between the Bornova Flysch Zone to the north and the Lycian nappes to the south (Şengör and Yılmaz 1981; Bozkurt and Mittwede 2005) (Fig. 1). The Alaşehir graben is one of the E-W trending prominent basins in western Turkey (Fig. 1). The graben consists of three faults in an E-W direction. The first fault, low-angle fault, the Alaşehir detachment, separates the hanging wall of sedimentary units of the Alaşehir graben from the footwall of metamorphic rocks and granodioritic intrusions (Işık et al. 2003). According to this study, the footwall of the Alaşehir detachment includes both ductile and brittle deformation. The tectonic evolution of the Alaşehir graben and its boundary faults were studied in detail by Seyitoğlu and Scott (1996), Temiz et al. (1998), Koçyiğit et al. (1999), Seyitoğlu et al. (2000), Yılmaz et al. (2000), Sözbilir (2001), Bozkurt and Sözbilir (2004), Çiftçi and Bozkurt (2009), Hakyemez et al. (2013), Poyraz et al. (2019). The geological structure of the Alaşehir graben was also investigated by geophysical tools (e.g., Eyidoğan and Jackson 1985; Gürer et al. 2002; Poyraz et al. 2019). Recently, the geothermal studies in the Alaşehir graben were also carried out by some scientists such as Erdogan and Candansayar (2017), Cambazoğlu et al. (2019), and Hacıoğlu et al. (2020). In addition to the mentioned studies, there are many geological (Akgün and Sözbilir 2001; Westaway et al. 2005; Koçyiğit 2005; Hançer 2013; Brogi et al. 2014) and geophysical (Sarı and Şalk 2006; Akyol et al. 2006; Bilim 2007; Irmak 2013; Kaypak and Gökkaya 2012; Altınoğlu et al. 2015) studies focused on the Denizli graben in the literature because of its complex tectonic structure with high seismic activity and its many hot springs, travertines, marbles, and archeologic sites.

Although many scientific studies mentioned

above were carried out by earth scientists with many geological and geophysical tools, the literature contains no detailed geological and geophysical study on the area between the Alaşehir and the Denizli grabens, and the subsurface structures of the area had not been defined in detail until now. Therefore, region by using gravity and seismic data (Fig. 1), we aimed to investigate the subsurface and seismo-tectonic structure of the region between the two main grabens of the Aegean extensional province where there is a tectonically very active.

The investigated region between 38.00° N–38.30° N latitude and 28.75° E–29.10° E longitude with an approximate area of about 1450 km² covers the area which includes the Sarıgöl district located in the southeast of the Alaşehir Graben and Buldan district located in the northwest of the Denizli graben shown in Fig. 1.

2 Geological Framework of the Study Area

The study area is located in the 'Aegean Extensional Province (AEP)' which extends from the Aegean Sea to central Anatolia (Fig. 1) (Bozkurt 2001; Koçyiğit 2005; Şengör 1979). The active faults of the AEP dominantly influence the Quaternary morphology of western Anatolia. Some studies (e.g., McKenzie 1978; Taymaz et al. 1991) indicate that the current extension oriented near N–S is occurring at a rate of 30 – 40 mm yr⁻¹ in the region. Additionally, to this, this oriented extension has replaced the Palaeocene orogenic contraction (e.g., Şengör et al. 1985, Taymaz et al. 1991; Seyitoğlu and Scott 1996; Bozkurt 2001). The existing system in this region resulted in developing a series of E–W-, NE–SW- and NW–SE-trending horst and graben structures (Bozkurt 2001; Kaymakçı 2006; Koçyiğit 2005; Koçyiğit and Deveci 2007; Şengör et al. 1985; Sözbilir 2002). Yılmaz et al. (2000) found that thick volcano sedimentary associations were formed within approximate N-S trending fault-bounded continental basins under an E–W extensional regime in the time range from the Early to Middle Miocene period. In addition to the E-W trending grabens, active normal faults were developed in the region. They are defined as neotectonic units. The study area shown in Fig. 1 is located at the junction point of these three main grabens and covers the southern end of Alaşehir graben and the northern end of the Denizli graben

between Sarigöl and Buldan districts.

Since the Late Triassic (230 million years ago), the Anatolia plate has been formed by the amalgamation of tiny island-arc terranes and platform carbonates during the closure of the Paleotethys and Neotethys oceans (Bozkurt 2001). The Alpine-Himalayan orogenic belt, which runs from the Alps in Western Europe to Southeast Asia, includes this plate. Due to this, the Turkish orogenic collage is made up of a number of Alpine tectono-stratigraphic units or terranes that formed in a variety of tectonic settings, including active and passive continental margins, rifts, arc and suture complexes, related to the opening and closing of numerous Neotethyan oceanic branches (Göncüoğlu 2010).

The detail tectonic structure of the Anatolian plate was not described because it was out of the scope of the study. However, due to the Sarigöl-Buldan region located in western Anatolia, important points relating to the tectonic evolution and geologic settings of western Anatolian were mentioned as possible here. Western Anatolia is known to be an area of widespread active continental extension (Bozkurt and Mittweide 2005) because it is mainly located in the convergent zone between the Africa, Arabia, and Eurasia plates (McKenzie 1972). The region has come into existence by the accretion of (semi-) rigid blocks to the southern margin of the Eurasian plate and it has undergone intense deformation (Özbakır et al. 2017).

The basement rocks of the study area are Paleozoic–Mesozoic, and Menderes massif metamorphic rocks are located between the Izmir-Ankara Neo-Tethyan Suture Zone to the north and the

Lycian Nappes to the south (Şengör and Yılmaz 1981). The Menderes Massif was exposed during the Early Miocene time according to Gessner et al. (2004) and is composed of various metamorphic rocks, which are mostly schists, quartzite and marbles, occasionally amphibolites and quartzites. The Alaşehir graben is ~150 km long, 3–40 km wide, E–W trending structure and forms one of the most prominent structural elements of western Turkey (Fig. 1 and Fig. 2). It is an actively growing asymmetric graben, with the active normal faults mainly located on the southern margin (Arpat and Bingöl 1969; Eyidoğan and Jackson 1985).

The Alaşehir graben was filled with Neogene-Quaternary sediments that are surrounded by horsts of the Menderes massif metamorphics (İztan and Yazman 1990; Yılmaz et al. 2000; Hakyemez et al. 2013). The Alaşehir graben’s faults lie in the NW-SE direction between the Salihli and Buldan districts. The Denizli graben is the southeast continuation of the main grabens of western Anatolia and has a length of 50 km and a width of 25 km that lies on a NW-SE direction - bounded by normal faults (Çakır 1999; Westaway 1990; Koçyiğit 2005). The graben is bounded by the Pamukkale fault zone in the NE, and the Babadağ fault in the SW. According to geological and seismic data, these faults are considered to be active. The Denizli Basin has opened in a NE-SW direction for 14 Ma (Westaway 1993). The Buldan horst has divided Denizli basin into two branches in the north with 2000 m high at the SW part of the study area. The geology map of the study area is shown on Fig. 2 in detail. The Denizli graben faults lie approximately parallel to the main faults of the Alaşehir graben.

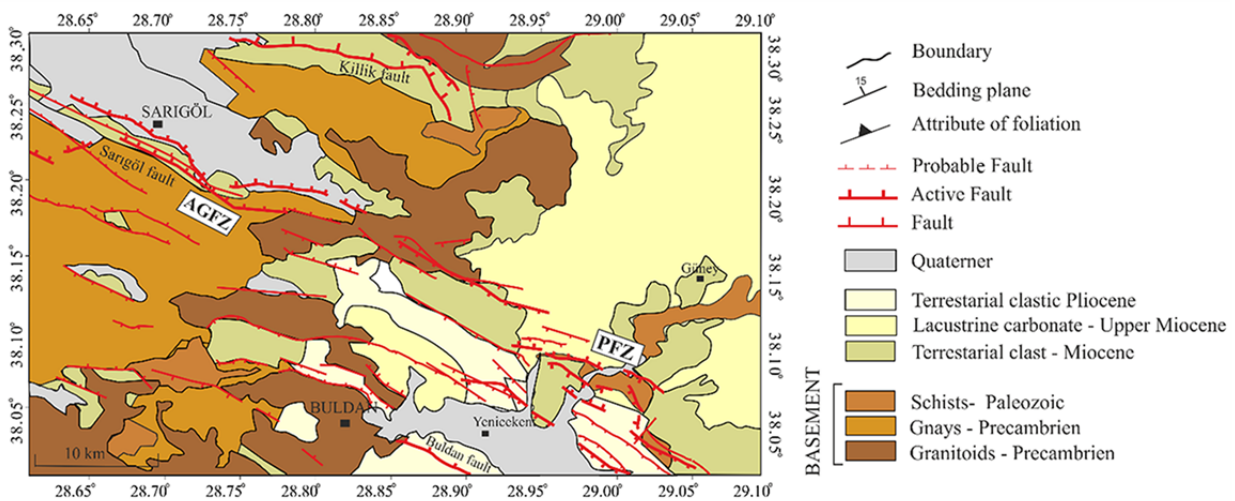


Fig. 2 Geology map of the study area, modified from MTA geology map <http://yerbilimleri.mta.gov.tr/home.aspx>, Akbaş et al. (2011) and Emre et al. (2013) PFZ: Pamukkale Fault Zone, AGFZ: Alaşehir Graben Fault Zone.

3 Seismicity Data and Analysis

In this study, in order to examine seismic activity of the region between 38.00° N–38.30° N latitude and 28.75° E–29.10° E longitude, a complete set of ~1500 earthquakes of $M_d \geq 1$ from 1970 to 2020 constructed from Bogazici University, Kandilli Observatory and Earthquake Research Institute, Regional Earthquake-Tsunami Monitoring Center (KOERI) catalogue, and T.C. Prime Ministry Disaster and Emergency Management was collected (Fig.3a). The seismic activity of the region is high. The high magnitude events between $4 \leq M_d \leq 6$ are located in between the Alaşehir and the Denizli grabens. Severely damaging earthquakes with $M_d=5.6, 5.2,$ and 5.0 occurred in the district of Buldan in July 2003. Additionally, we observed that earthquakes with magnitude $M_b \geq 5.0$ intensively occurred along the Pamukkale Fault Zone. The major of seismic activity as seen in Fig. 3a clustered along the intersection region between the AGFZ and the PFZ. Fig. 3b indicates depth distribution of the number of earthquakes occurred in the region. Their depth range of the events varied from 5 and 10 km. At the first

stage, to ensure the integrity of the dataset, the whole dataset was converted to local magnitude by using the formula $ML = (0.9897 * M_d) + 0.0978$ (Kalafat 2016), ($R^2 = 0.8955$; Cohesion coefficient). At the second stage, the declustering process based on Reasenbergs (1985) method was applied to remove artificial (unnatural) seismic events relating to artificial quarry blasts and mine blasts. Therefore, ~5 percent of all data was thrown out. To investigate the seismic activity of a region, seismic parameters (Gutenberg-Richter value (b -), seismic activity rate (a -), and Magnitude of completeness (M_c)) are estimated by many statistical methods (e.g., Öztürk 2018; Polat 2022). In such studies, the Gutenberg-Richter (GR) law is usually used. In this approach, the frequency of earthquake occurrence is described as a function of the magnitude. To estimate the b - and a - values, the formula below is used:

$$\log N = a - bM \tag{1}$$

In Eq.(1), $N(ML)$ is the number of earthquakes with a magnitude larger than M per year; a and b are the constant parameters. The b -value is the slope of the frequency-magnitude distribution and related to the distribution of stress and strain (Utsu 1965;

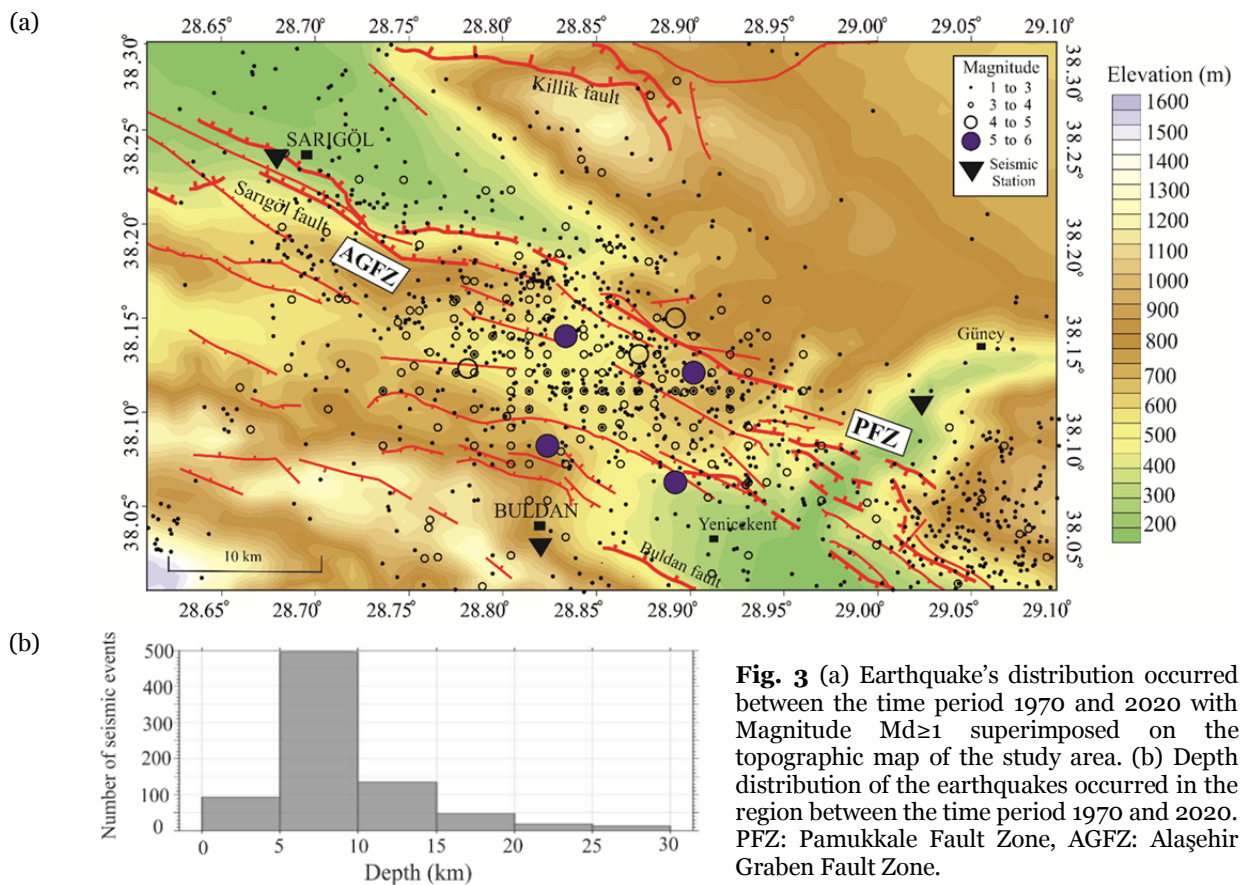


Fig. 3 (a) Earthquake’s distribution occurred between the time period 1970 and 2020 with Magnitude $M_d \geq 1$ superimposed on the topographic map of the study area. (b) Depth distribution of the earthquakes occurred in the region between the time period 1970 and 2020. PFZ: Pamukkale Fault Zone, AGFZ: Alaşehir Graben Fault Zone.

Scholz 1968), the material heterogeneity, thermal gradient, volcanic activity, tectonic events in the Earth's crust (e.g., Warren and Latham 1970; Katsumata 2006). The a - and b -values represent the generalized 'fractal dimension' of earthquake magnitude distributions (Gutenberg and Richter 1955). This estimation is based on a fractal relation between frequency of occurrence and the radiated energy, seismic moment, and fault length. The estimated parameters are very significant because they can provide useful information about earthquake behaviour and fault zone orientation (Turcotte 1986). The estimated M_c parameter changes over time depending on the number of seismic stations deployed in the investigated region and the techniques of investigation (Ahadov and Ozturk 2022). The b -value is the slope of the Frequency-Magnitude Distribution (FMD). Generally, it is used to provide a relative measure of the likelihood of large and small magnitude seismicity of the investigated area. A dislocation model for the seismic source (Gutenberg and Richter 1955) is assumed in its interpretation. Then, Turcotte (1986) indicated that a scale-invariant recurrence interval was also required. The seismic activity rate is generally defined with a -value. It represents the intercept acquired from the FMD analysis.

Spatial variations of the seismic parameter for the earthquake occurrences in the region shown on Fig. 1 were investigated in this study. For this purpose, ZMAP software (Wiemer 2001) was applied to the integrated and declustered data constructed in this study. For calculating the b -value, the maximum likelihood method was used (Aki 1965; Bender 1983; Utsu 1999). This method is defined as:

$$b = \frac{\log(e)}{\sum_{i=1}^N \frac{M_i}{N} - M_c} \quad (2)$$

In this equation, e , M_c , N are the base of natural logarithm ($e = 2.1718$), the completeness magnitude, and number of earthquakes, respectively. The seismicity parameters were calculated at each grid node of 1 km along both latitude and longitude.

4 Gravity Data and Analysis

Gravity data is commonly used in tectonic structure investigation (Yuan et al. 2012; Selim 2016; Sainz-Maza et al. 2017; Bora et al. 2018; Uwiduhaye et al. 2018; Bba et al. 2019; Dilalos et al. 2019;

Kanthiya et al. 2019; Kebede et al. 2021). The complete Bouguer gravity anomaly data of the study area was obtained from the General Directorate of the Mineral Research and Exploration (MTA) of Turkey. The data was collected with a 0.1 mGal accuracy at 250–500 m station spacing and then gridded over a 1 km² area. The data was tied to the Potsdam (981260.00 mGal) base value. All necessary corrections were made by MTA. The Bouguer correction was done for a density of 2.40 g cm⁻³. The contour map of Bouguer gravity anomaly data of the study area is shown in Fig. 4a, with the anomaly values ranging from -34 to 12 mGal.

It is well-known that Bouguer gravity anomaly data presents the whole effect of shallow and deep sources. Therefore, as dealing with shallower local geological structures, the deeper sources effects should be removed. In this study, frequency domain filtering was used to remove the deeper sources effects from shallower local geological structures. The radially averaged power spectrum of gravity data was calculated, and a Butterworth low pass filter was applied to gravity anomaly data (Altinoğlu et al. 2015, 2018; Altinoğlu 2019) to enhance the regional gravity data with cut-off frequency ($k_c=0.409$ Hz). Then, the residual gravity anomaly data was obtained by subtracting the regional anomaly data from the gravity data. The residual gravity anomaly map is given in Fig. 4b.

In potential field applications, defining the boundaries of the causative body that causes gravity anomalies is an important problem. To solve this problem, many derivative-based edge detection techniques were commonly used in previous studies (Verduzco et al. 2004; Cooper and Cowan 2006; Ma and Li 2012; Ferreira et al. 2013; Zhou et al. 2013; Yuan et al. 2014; Wang et al. 2014; Wang et al. 2015; Du et al. 2017; Rezaie et al. 2017; Wang et al. 2017). The edge detection techniques comprised of the horizontal gradient, tilt angle and theta map techniques were used in this study. Although the horizontal gradient method (Blakely 1995; Cordell 1979; Cordell and Grauch 1985) is the oldest, it is widely used as one of the edge detection techniques to define the boundaries of density contrast and magnetic susceptibility from the potential field data.

At the edges of the subsurface source body, the horizontal gradient magnitude and the analytical signal indicate that gravity values become maximum. According to Miller and Singh (1994), the maximum

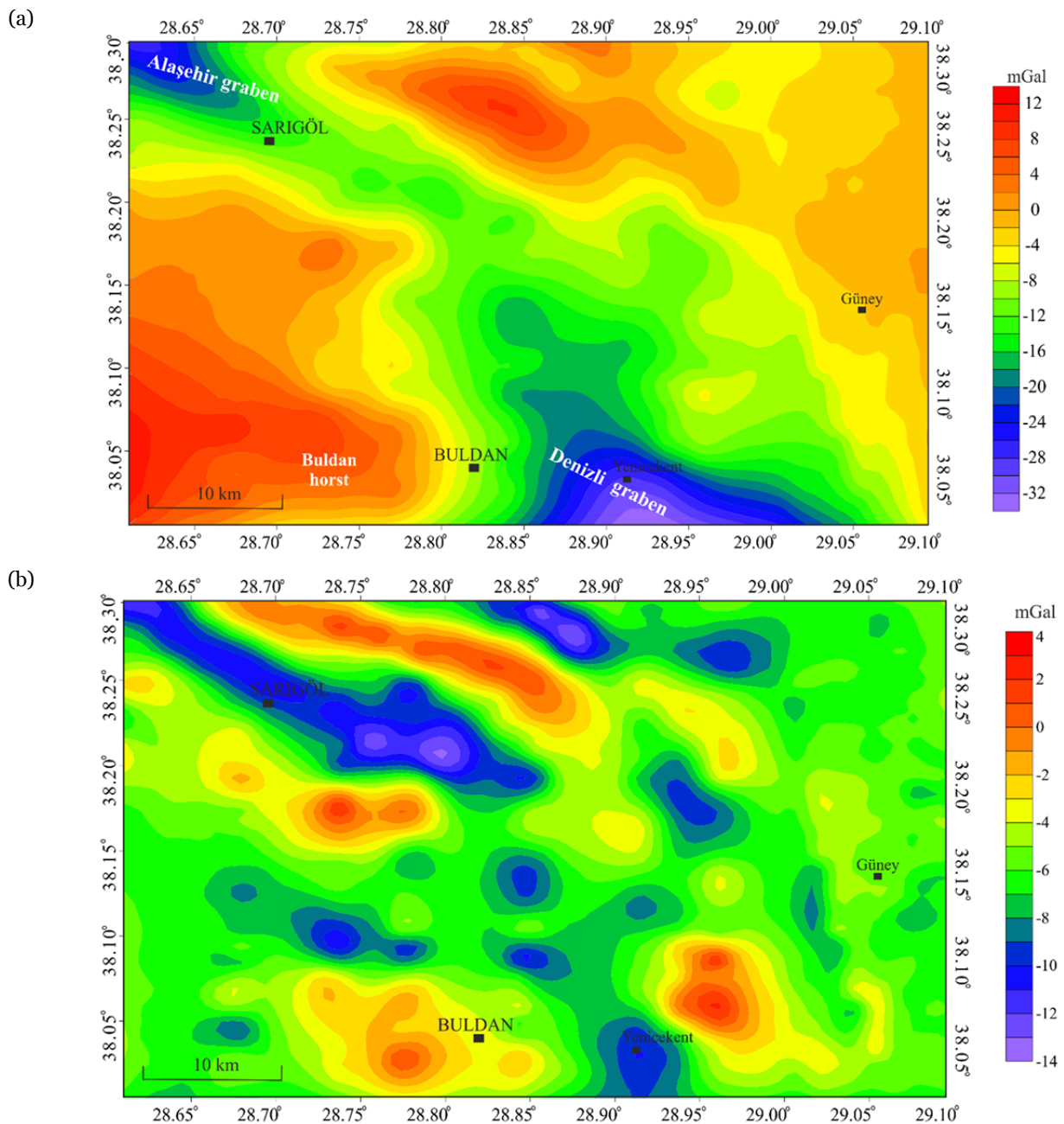


Fig. 4 (a) Bouguer gravity anomaly map of the study area. (b) Residual gravity anomaly map of the study area with 2 mGal contour interval.

values of horizontal gradient magnitude and analytic signal suggest the edges of the subsurface causative body.

The amplitude of the horizontal gradient magnitude is expressed as follows (Blakely and Simpson 1986):

$$HG = \sqrt{\left(\frac{\partial g}{\partial x}\right)^2 + \left(\frac{\partial g}{\partial y}\right)^2} \quad (3)$$

where g is the gravity field anomaly and $\partial g/\partial x$ and

$\partial g/\partial y$ are the horizontal derivatives of the anomaly.

The tilt angle method (Miller and Singh 1994) based on the relation between vertical and horizontal derivatives was additionally used to find out the source boundaries because of zero values. Over a source, the tilt angle becomes usually positive. Thus, zero values reflect the source edges (Miller and Singh 1994). This method can be also used to improve the edges of anomalies in shallow and deep sources.

$$TA = \tan^{-1} \left[\frac{\frac{\partial g}{\partial z}}{\sqrt{\left(\frac{\partial g}{\partial x}\right)^2 + \left(\frac{\partial g}{\partial y}\right)^2}} \right] \quad (4)$$

Wijns et al. (2005) proposed the theta map method that is the normalization of horizontal gradient because the maxima of the theta map correspond to the source edge (Wijns et al. 2005; Cooper and Cowan 2008).

$$Theta = \frac{\sqrt{\left(\frac{\partial g}{\partial x}\right)^2 + \left(\frac{\partial g}{\partial y}\right)^2}}{\sqrt{\left(\frac{\partial g}{\partial x}\right)^2 + \left(\frac{\partial g}{\partial y}\right)^2 + \left(\frac{\partial g}{\partial z}\right)^2}} \quad (5)$$

Because of these, the horizontal gradient, the tilt angle, and the theta map edge detection methods were applied to the residual gravity map to determine the buried structural boundaries and discontinuities in the investigated region.

To image the sediment basement relief, 3-D inversion of gravity data was analyzed by using a code developed by Pham et al. (2018). This code uses an advanced iterative rapid approach based on a combination of Granser's FFT-based algorithm and Cordell and Henderson's space domain technique. The inversion approach does not require a mean depth or low-pass filtering.

The gravitational anomaly of a sedimentary basin was defined by Granser (1987) as follows:

$$\Delta g = F^{-1} \left[2\pi\gamma\Delta\rho_0 \frac{1}{|k|+\lambda} \left(F[1 - e^{-\lambda h}] - \sum_{n=1}^{\infty} \frac{(-|k|)^n}{n!} F[e^{-\lambda h} h^n] \right) \right] \quad (6)$$

Eq. (6) is reduced to (Granser, 1987) in the case of the gravity effect of an infinite horizontal slab (Bouguer slab) with a top at surface and a slab bottom at a depth h:

$$\Delta g = \frac{2\pi\gamma\Delta\rho_0}{\lambda} (1 - e^{-\lambda h}) \quad (7)$$

Granser (1987) proposed using the mean depth of the basement interface as a reference level z_0 to increase the convergence speed of the forward algorithm in Eq. (6), in the sense that the depth of the interface is described by $h=z_0 + h$. The use of a reference level z_0 , according to Granser (1987) requires an additional Bouguer slab term and an upward continuation from the level z_0 to the surface.

As a result, (Granser 1987) becomes Eq. (6):

$$\Delta g = \frac{2\pi\gamma\Delta\rho_0}{\lambda} (1 - e^{-\lambda z_0}) + 2\pi\gamma\Delta\rho_0 e^{-\lambda z_0} \times F^{-1} \left[\frac{e^{-|k|z_0}}{|k|+\lambda} \left(F[1 - e^{(-\lambda\Delta h)}] - \sum_{n=1}^{\infty} \frac{(-|k|)^n}{n!} F[1 - e^{-\lambda\Delta h} \Delta h^n] \right) \right] \quad (8)$$

Another iterative inversion approach based on the Bouguer slab formula was developed by Cordell and Henderson (1968). In the space domain, this procedure is simple to compute. The density contrast is considered to be uniform in Cordell and Henderson's (1968) algorithm. It varies with depth in our algorithm.

Iterations start with a rough estimate of the depth of the interface $h(x, y)$. An endless slab is thought to be generating the observed anomaly at each grid point). According to Cordell (1973), the equation for the infinite horizontal slab (Eq. (7)) yields the first approximation of the depth to the basement with exponential density contrast variation:

$$h_{(i,j)}^1 = -\frac{1}{\lambda} \ln \left(1 - \frac{\lambda \Delta g_{obs(i,j)}}{2\pi\gamma\Delta\rho_0} \right) \quad (9)$$

The gravity anomaly of the sedimentary basin is then determined at each observation site using the Granser (1987) technique, which is considerably simpler and takes less computer time than the Cordell and Henderson (1968) algorithm, which is based on the segmentation of the basin into prisms. For the next modification or refinement of the model, Cordell and Henderson (1968) suggested the following relationship:

$$h_{(i,j)}^{(t+1)} = \frac{\Delta g_{obs(i,j)}}{\Delta g_{calc(i,j)}^{(t)}} h_{(i,j)}^{(t)} \quad (10)$$

$g_{calc}(i, j)$ is the estimated gravity anomaly at grid point (i, j) , and t is the number of iterations. Instead of using an infinite-slab approximation such as in Bott's method (1960), the above ratio is utilized to revise the bottom depths of prisms.

The gravity anomalies of the iterated model are recalculated when each thickness element is iterated, and another iteration is conducted. After each iteration, the mean depth of the basement interface is redefined. In gravity inversion, the iterative procedure aims to reduce the difference between the calculated and observed anomaly. When a desired fit between $g_{obs}(i, j)$ and $g_{calc}(i, j)$ is achieved for each grid point (i, j) , the model is satisfied.

The proposed approach enables rapid and accurate computation while maintaining convergence since it combines forward modelling in the frequency domain and iterative inversion in the space domain. In the inversion process, the code does not require a mean depth or filter. In the process, the density contrast ($\Delta\rho$) of 0.3 g/cm³ between Neogene sedimentary fill (~2.4 g/cm³) and metamorphic complex (~2.7 g/cm³) and decay constant (λ) of 0.001

g/cm³ are taken.

5 Results

Seismic parameters (M_c , a -, and b -values) for this region were calculated by using ZMAP software. The seismic parameters, including M_c , a -value and b -value, were found as 2.8, 6.657, and 1.58, respectively (Fig. 5a). As calculating M_c -value by using the frequency-magnitude distribution of earthquakes (Wiemer and Wyss 2000), M_c -value was defined as the minimum magnitude of complete recording. According to the FMD, Gutenberg-Richter relation was found as $\log N = 6.657 - 1.58ML$. The b -value map is shown in Fig. 5b. We detected that b -values range between 0.2 and 2. The distribution of b -value errors in the study area is shown in Fig. 6. The horizontal gradient map residual gravity anomaly data (Fig. 7a) highlights a number of lineaments in NW-SE and W-E directions that represent the major structural trends. The zero contours of the tilt angle map indicate the density discontinuities and are given by white contours in Fig. 7b. The zero contours of the tilt angle fit perfectly with the result of the horizontal gradient. The maximum values of the theta map also represent the density discontinuities. The common density discontinuities enhanced from both horizontal gradient and tilt angle maps are drawn by black lines in the theta map (Fig. 7c) and seen that they were located in the maximum values of the theta map. These lineaments are proposed as the lineament structures of the study area. The basement relief map with the enhanced lineaments is given in Fig. 8; the general regional NW-SE direction tectonic trend can be seen easily. The sediment basement topography ranges between 0.1 and 2.1 km. All the reliefs in the sediment topography map (Fig. 8) are bounded with the lineaments defined by the edge detection process. The defined lineaments corresponding to the sedimentary topography and some newly buried

lineaments were defined, which are covered by young sediment deposits. The superimposition of the earthquake epicenters on a new tectonic lineament map for the study area is given in Fig. 9.

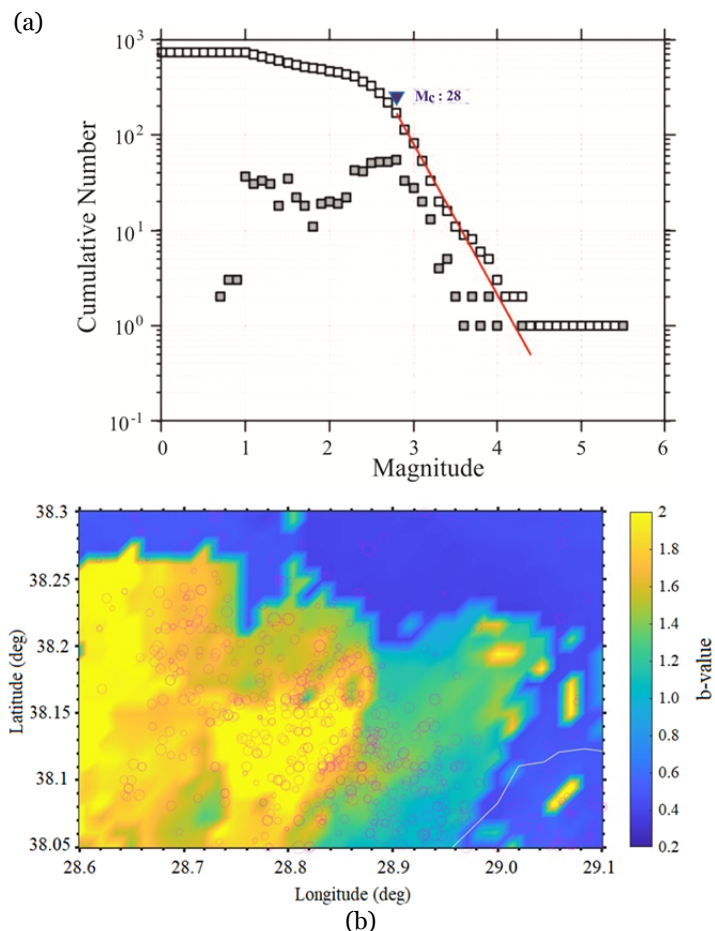


Fig. 5 (a) Frequency magnitude distribution of the declustering catalogue. Plotted is both the cumulative (squares filled in white) and non-cumulative form (squares filled in gray); (b) b -value map of the region between Sarigöl and Buldan districts for the period 1970-2020.

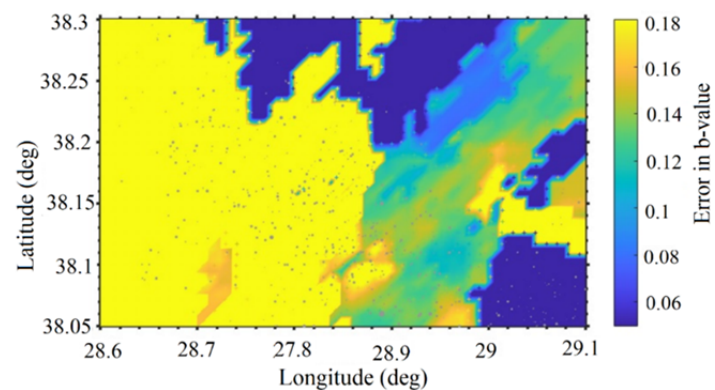


Fig. 6 Standard deviation of b -value for the study area.

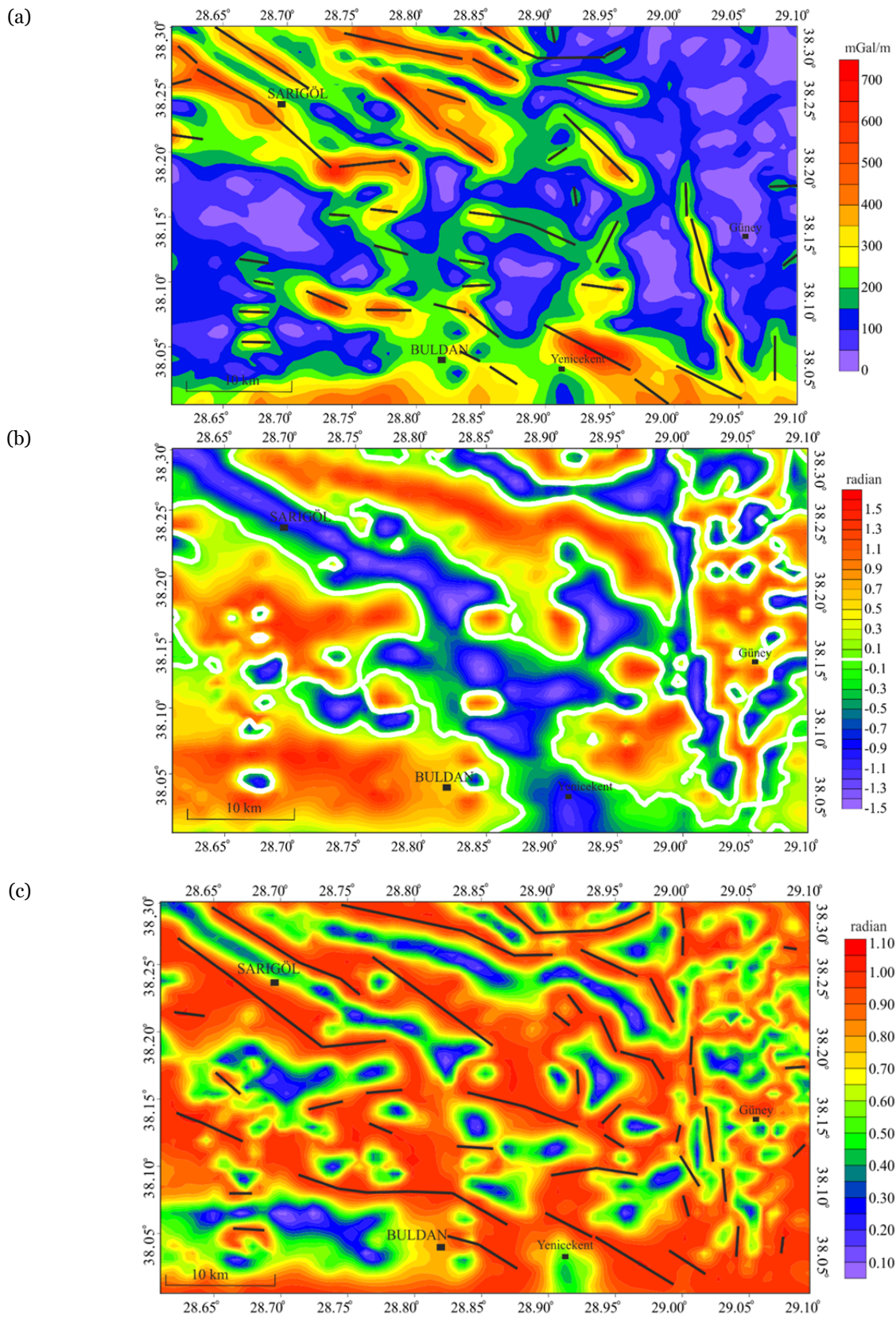


Fig. 7 (a) Horizontal gradient gravity map of the study area (black lineaments correspond to density discontinuities); (b) Tilt angle map of the study area, zero contours were drawn by white color which represent the density discontinuities. (c) Theta map of residual gravity anomaly map of the study area (black lineaments represent the common lineaments in horizontal gradient and tilt angle maps).

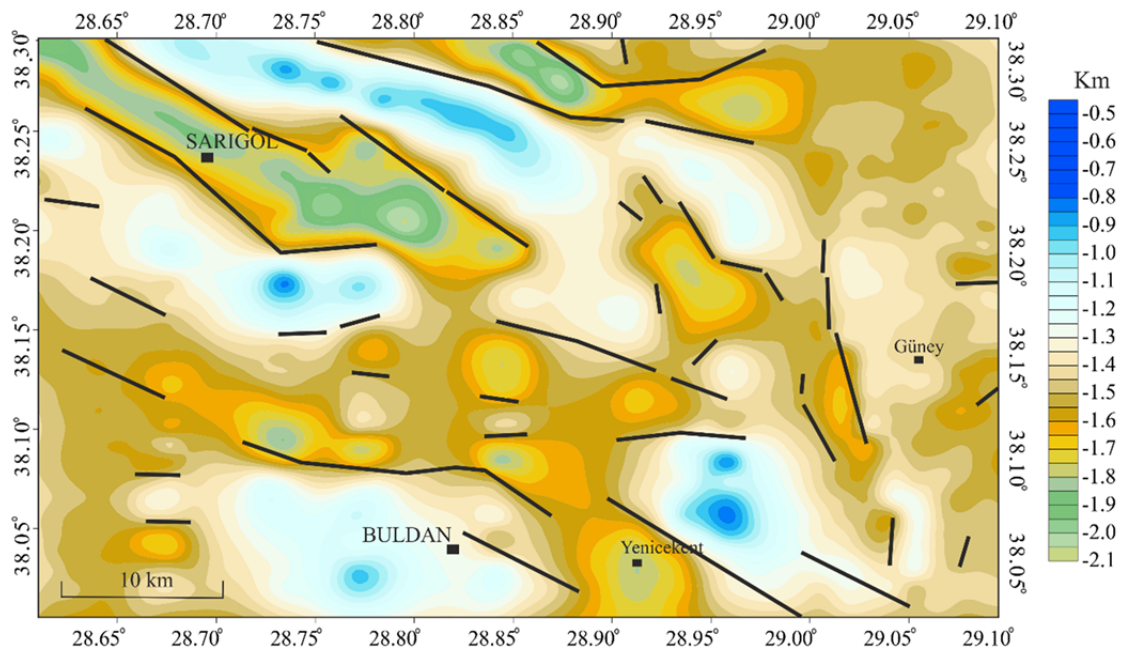


Fig. 8 Sediment basement relief map enhanced by 3D inversion of gravity data of the study area. The estimated lineaments by edge detection techniques of gravity data were shown by black lines.

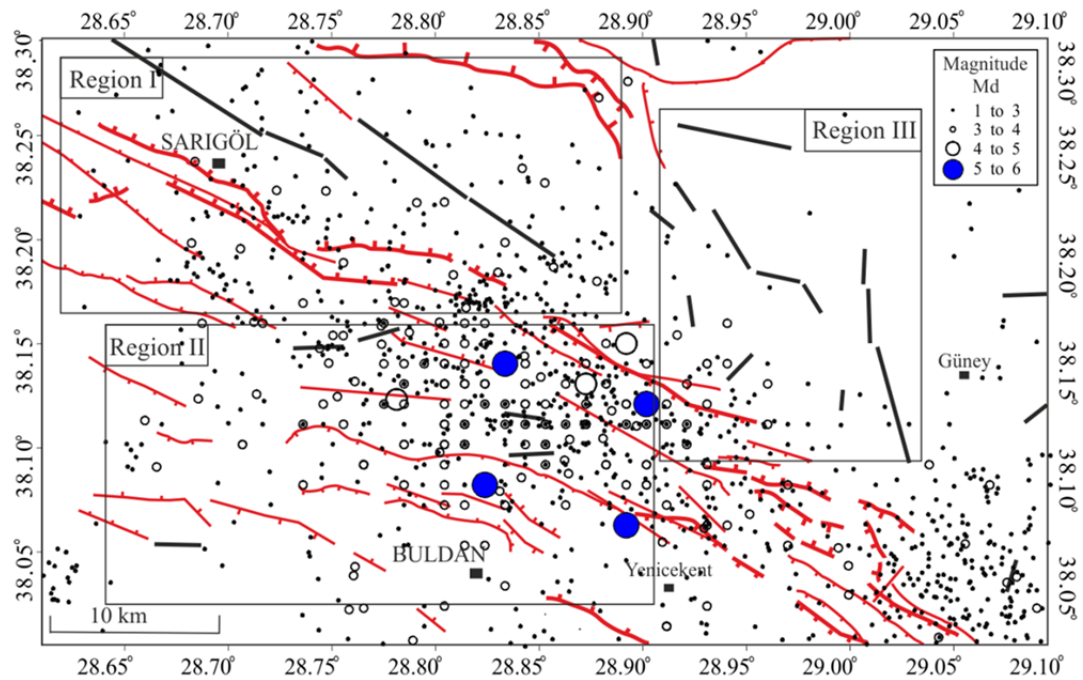


Fig. 9 New lineament map of the study area superimposed on earthquake distribution map from 1970 to 2020, the known faults of the area in red and the new proposed lineaments in black color. PFZ: Pamukkale Fault Zone, AGFZ: Alaşehir Graben Fault Zone. Black rectangulars denote the location of the local areas.

6 Discussion

Based on the obtained results from the seismic hazard analysis in this study, the seismic hazard risk

of the region was revealed. For this region, a-value calculated as 6.657 is related to earthquake activity level of the studied region. It means that this value changes as a function of the length of the study area,

time period of the catalog as well as the number of earthquakes. The Mc-value calculated as 2.8 is a significant parameter for statistical seismicity studies. This value depends on magnitude levels of the earthquakes in the catalogue. Therefore, the high-quality parameters were estimated by using the earthquake catalogue created with the maximum number of earthquakes.

The derived b-value from this analysis is 1.58. With b ranging from 0.2 to 2, there were notable variations in the b-value. Changes in b-value depend on many factors. The relative numbers of small aftershocks caused by large earthquakes or swarms result in variations in b-value. In addition to the factors, rock fractures also cause a noticeable decrease in b-value. It is probably related to an increase in shear stress and a reduction in restricted compression (Öztürk and Gerdan 2020). Moreover, apart from these reasons, there are some factors such as thermal gradient, crack density, fault length, geological complexity, slip distribution, material properties and strain circumstances (e.g., Mogi 1962; Scholz 1968). The b-value map in Fig. 5b indicates a clear high heterogeneity in the region, with low b-values predominating. Also, an anomaly of b-value higher than 1 was detected within the segment of the Alasehir Graben Fault Zone (AGFZ) between Sarigöl and Buldan districts. Previous studies (e.g., Öncel et al. 2001; Öncel and Wilson 2002) indicated that regional-scale estimates of b-value generally range between 0.5 and 1.5. On the other hand, on average, the b-value for the regional scale is ~ 1 (Frohlich and Davis 1993; Jackson and Kagan 1999). Higher b-values were observed in the Buldan horst and surrounding area. In contrast, lower b-values were observed in the northeast part of the interaction region between the Denizli and the Alaşehir grabens. The low b-values in the NE part of the intersection between the Alaşehir graben and the Denizli graben were well-correlated with the high Bouguer anomalies (Fig. 4a). This observation seems consistent with the results of Polat et al. (2008) obtained from the Aegean region. They interpreted these areas in asperities as expressions of stress levels and high-stress accumulation, which probably cause lower b-values. Maybe, the lower b-value was caused by the brittle-ductile transition induced by the increase in confining pressure (Amitrano 2003).

Another reason for this is that positive Bouguer anomaly values as high as +10 mGal and low b-values

are probably related to a thinner crustal root. Both explanations need more data to be justified. In comparison, negative Bouguer anomaly values were observed in the Alasehir and the Denizli grabens. Also, in these grabens, intermediate to high b-values were found. This suggests that there is a relation between gravity anomaly and b-value. This relation is strongly related to the active fault mechanism existing in the region. Additionally, the distribution of b-value errors in the study area is mapped in Fig. 6. An error interval in the b-value is not high because there is a small change between maximum and minimum values, which are 0.18 and 0.05, respectively. The error interval in the b-value was not considered for the whole study area except for the Buldan horst on small-scale deviations. However, a similar pattern was not observed in the Buldan horst. This may be related to the Buldan horst having low-stress levels, even though the intensity of microearthquakes is high in this region. In both laboratory testing and field investigations, low b-values were associated with high-stress situations (Wyss and Matsumura 2002). It is often tied to low b-values and can be associated with Bouguer gravity anomaly (Wilson and Kato 1992, 1995; Khan 2005). Sarı and Şalk (2006) investigated the gravity anomaly of the Aegean region in detail, finding that high Bouguer anomalies in the Aegean Extension Region correspond to low b-value areas. (Polat et al. 2008). They interpreted these areas in asperities as expressions of stress levels and high-stress accumulation, which probably cause lower b-values. After declustering, we observed that many micro and local earthquakes were caused by intermediate earthquakes that occurred in the region between the NW segment of the PFZ and the SE segment of the AGFZ (Fig. 3a).

The NW-SE trending low gravity anomalies in the residual gravity map (Fig. 4b) were observed in the northwest and the southeast parts of the study area that represent the low-density Quaternary and Neogene units, while the maximum high anomalies located in the outer sides of the basins reflect the effect of high-density Menderes massif basement rocks. The residual gravity map correlates in a good manner with the geological map of the coverage area and the general regional trend. The positive gravity anomalies imply high-density metamorphics, which developed in the western and eastern sides of the Denizli and Alaşehir basins and are hosted in the Buldan horst. The negative gravity anomalies suggest

the low-density sedimentary deposits developed in the Denizli and Alaşehir grabens. The linear tectonic structures of the study area such as faults were defined by the edge detection methods applied to the gravity anomaly data. The tilt angle (Fig. 7b) and theta map (Fig. 7c) of the gravity map give detailed information about the lineaments of the region. The new lineaments are mainly NW-SE direction that reflect the main geo-structural trend of the study area (Fig. 8). To better understand the tectonic structure and shallow subsurface features, the sediment basement topography was modelled from residual gravity anomaly data by using a code modified by Pham et al. (2018). The maximum depth levels ranging from 2- 2.1 km were observed in the Alaşehir graben and the Denizli graben, as exhibited in Fig. 8. The thickness of sediment deposits is defined as 2 km in the southern part of the Alaşehir basin. In this study, this result coincides with previous studies; Paton (1992) indicated the sediment thickness as 1.3-1.4 km between Alaşehir and Salihli districts where the area is located at the north of the study area; Gürer (2002) determined the sediment thickness as 0.9- 3.5 km for Alaşehir graben from the magnetotelluric study; Bozkurt and Sözbilir (2004) defined it as 1.3-1.4 km and Purvis and Robertson (2005) as 1km from geological studies; Sarı and Şalk (2006) stated 1.5-2 km sediment thickness for the Alaşehir graben from gravity data and Yılmaz and Gelişli (2003) found it as 2-2.5 km from seismic sections in the Alaşehir graben. In the northwestern part of the Denizli basin, the thickness of sediment deposits was determined as 2 km. These findings are consistent with earlier research: Turgay et al. (1980) indicated 2 km depth for the basement in the Sarayköy-Denizli areas using geoelectric studies, Sarı and Şalk (2006) found the sediment thickness to be 1.5-2 km in the northern part of the Denizli basin via gravity studies and Altınoğlu (2012) defined the sediment thickness varied between 2-3 km for the Denizli basin using gravity studies. The sediment basement relief map (Fig. 8) exhibits that the Denizli basin structure lies to the Alaşehir basin in NW-SE direction that is divided into three branches, and each of them is bounded by Menderes metamorphic basement rocks. As seen in Fig. 9, most of the lineaments obtained from the edge detection maps are consistent with the active fault map of MTA (2003). These are main faults in the AGFZ as Sargöl fault and the Killık fault in the NW part of the study

area and the faults located in the PFZ. Many new lineaments were detected as a result of this study that do not exist in the MTA active fault map of the region (Fig. 1), and some of them are probably buried faults. The most important one is probably a buried fault which lies in the NW-SE direction through the Alaşehir graben (Fig. 9). These possibly buried faults were covered by low-density Neogene sediments; so no geological or morphologic trace can be found but can be discovered by geophysical studies. The new lineament map of the study area is superimposed on the earthquake distribution map from 1970 to 2020 and given in Fig. 9. The new proposed lineaments are shown with black lines in Fig. 9. The general trend is NW-SE direction is consistent with the regional tectonic trend. The earthquake distribution, as shown on the map, supports the new lineaments determined in this study. A seismic cluster area is shown in NW-SE direction on the area between the Alaşehir and the Denizli grabens.

The lineaments map of the region shown in Fig. 9 are mostly reflecting the NW-SE trending tectonic structure of the region (Fig. 1). The new lineaments in Region I are remarkably consistent with the dominant directions of regional faults. Although the lengths of the new lineaments in Region II are not as large as the Region I, the new lineaments detected in small sizes are compatible with a slight deviation with the fault orientation of the region. In contrast to this, we cannot compare the new lineaments with faults located in Region III because of the lack of faults in the region. The seismic activity of Region III seems weak in contrast to Region II. Most of the earthquakes occur along the AGFZ and the PFZ shown on Fig. 3a. It suggests that their epicentres are located in the interior part of the western part of the Anatolian plate because they are far away from the boundary of tectonic plates. This is probably related to the number of seismic stations. In the whole study region, there are three permanent seismic stations. Due to this, micro events which have occurred in this region do not seem to exist. The seismic activity is so high in the Region II. The observed seismic activity is probably caused by the known faults because their lengths are greater than new lineaments. In other words, relative lengths of the new lineaments are too small compared to known faults in the region (Fig. 9). All lineaments comprising new and previously detected faults in Region I and II are likely related to the graben and uplift formations because the upper

crust beneath the Anatolian plate is being pulled apart by north–south extensional stresses resulting from slab rollback, where the African plate is subducting northwards beneath Eurasia while the slab is sinking by gravitational forces causing it to retreat southwards (e. g., Meng et al. 2021). This active system may trigger the faults to be seismically active due to the system causing increase in the stress accumulation in and around the faults. This finding, we thought, is to explain why the observed seismic activity in the region is currently high (Fig. 9) and most earthquakes occur in the upper crust. Due to the findings from this study, it may be claimed that the non-uniform uplift regime affects variations in the thickness of the graben and basements shown in Fig. 8.

7 Conclusion

To examine the continuity of the subsurface fault structure of the Sargöl- Buldan region, Western Anatolia, we have used gravity and seismicity data. The horizontal gradient, the tilt angle, and the theta map edge detection methods were applied to the residual gravity map to reveal the subsurface structural boundaries and discontinuities in the investigated region. As seen in Fig. 9, new lineament zones detected in Region I are close to the district of Sarıgöl and surrounding area. Observed features of the derivatives are closely compatible with the surface fault structure of the AGFZ and the PFZ. In addition to this, to improve the findings by using gravity analysis, seismic parameters of the region were also determined. This study certainly indicates that combining gravity anomalies and their derivatives with seismic study are useful in illustrating subsurface fault structures and comparing their coseismic activities. Derived main results from this study are briefly listed as follows:

- Shallow subsurface structure of the study

References

- Ahadov B, Öztürk S (2022) Spatial variations of fundamental seismotectonic parameters for the earthquake occurrences in the Eastern Mediterranean and Caucasus. *Nat Hazards* 111: 2177-2192
<https://doi.org/10.1007/s11069-021-05170-1>
 Akbaş B, Akdeniz N, Aksay A, et al. (2011) 1:1.250.000 ölçekli Türkiye Jeoloji Haritası. Maden Tetkik ve Arama Genel

area is delineated by using gravity data.

- Edge detection methods were applied to Gravity data to identify new new lineaments.
- Additionally, a -, b - values and M_c have been calculated by using seismicity data.
- Identified new lineament parallel to the northern boundary of the Alaşehir graben in the Region I is probably a buried fault which is compatible with the regional geological trend and seismicity of the region.
- In the Region II, we cannot compare the new lineaments with the seismic activity due to lack of sufficient seismic stations. In addition to this, their lengths are too small to produce intermediate earthquakes.
- In Region III, there is no correlation between the new lineaments and the regional geological trend and seismicity of the region because of no seismic activity and traces of the surface fault. In Region III, a lower- b value was found. This may be related to the brittle-ductile transition induced by the increase in confining pressure.
- We suggest a correlation between positive Bouguer value and low b -values, which are associated with thin crust. Negative Bouguer values are correlated with high b -values associated with relatively thicker sediments of graben. It is proposed that low b -values may correspond to high-stress accumulation zones and may represent locales for future earthquake. These values are helpful in preparation of a seismic hazard map.

Acknowledgments

We would like to thank Prof. Dr. Tekin Yürür for improving our manuscript related to the structural geology of the study area. We also thank the anonymous reviewers for their valuable time and comments in the development of the publication.

- Müdürlüğü Yayını, Ankara, Türkiye.
<http://yerbilimleri.mta.gov.tr/home.aspx> (Accessed on 7 February 2022)
 Aki K (1965) Maximum likelihood estimate of b in the formula $\log(N)=a-bM$ and its confidence limits. *Bull Earthquake Res Inst Univ Tokyo* 43: 237-239.
 Akgün F, Sozibilir H (2001) A palynostratigraphic approach to

- the SW Anatolian molasse basin: Kale-Tavas molasse and Denizli molasse. *Geodin Acta* 14: 71-93.
<https://doi.org/10.1080/09853111.2001.11432436>
- Akyol N, Zhu LM, Sözbilir H, Kekovalı K (2006) Crustal structure and local seismicity in western Anatolia. *Geophys J Int* 16: 1259-1269.
<https://doi.org/10.1111/j.1365-246X.2006.03053.x>
- Altinoğlu FF (2012) Investigation of tectonics of Western Anatolia by geophysical methods. PhD thesis, University of Pamukkale, Denizli. p 225.
- Altinoğlu FF, Sari M, Aydın A (2015) Detection of lineaments in Denizli basin of western Anatolia region using Bouguer gravity data. *Pure Appl Geophys* 172(2): 415-425.
<https://doi.org/10.1007/s00024-014-0911-y>
- Altinoğlu FF, Sari M, Aydın A (2018) Shallow crust structure of the Büyük Menderes graben through an analysis of gravity data. *Turkish J Earth Sci* 27(6): 421-431.
<https://doi.org/10.3906/yer-1712-6>
- Altinoğlu FF (2019) Determination of linear features of Elazığ province and surrounding by applying boundary analyzing techniques to gravity data (In Turkish) Pamukkale Üni Müh Bil Derg 25(6): 785-793. .
<https://doi.org/10.5505/pajes.2018.50469>
- Amitrano D (2003) Brittle - ductile transition and associated seismicity: Experimental and numerical studies and relationship with the b value. *J Geophys Res Solid Earth* 108(B1).
<https://doi.org/10.1029/2001JB000680>
- Arpat E, Bingöl E. (1969) The rift system of the western Turkey; thoughts on its development. *Bull Miner Res Expl* 78: 33-39.
- Bba AN, Boujamaoui M, Amiri A, et al. (2019) Structural modeling of the hidden parts of a Paleozoic belt: Insights from gravity and aeromagnetic data (Tadla Basin and Phosphates Plateau, Morocco). *J Afr Earth Sci* 151: 506-522.
<https://doi.org/10.1016/j.jafrearsci.2018.09.007>
- Bender B (1983) Maximum likelihood estimation of b values for magnitude grouped data. *Bull Seismol Soc Am* 73(3): 831-851.
<https://doi.org/10.1785/BSSA0730030831>
- Bilim F (2007) Investigation into the lineaments and thermal structure of Kütahya-Denizli Region, Western Anatolia, from using aeromagnetic, gravity and seismological data. *Phys Earth Planet Int* 165: 35-146.
<https://doi.org/10.1016/j.pepi.2007.08.007>
- Blakely RJ (1995) *Potential Theory in Gravity and Magnetic Applications*. Cambridge University, Cambridge.
<https://doi.org/10.1017/CBO9780511549816>
- Blakely RJ, Simpson RW (1986) Approximating edges of source bodies from magnetic or gravity anomalies. *Geophysics* 51(7): 1494-1498.
<https://doi.org/10.1190/1.1442197>
- Bora DK, Borah K, Mahanta R, et al. (2018) Seismic b-values and its correlation with seismic moment and Bouguer gravity anomaly over Indo-Burma ranges of northeast India: Tectonic implications. *Tectonophysics* 728: 130-141.
<https://doi.org/10.1016/j.tecto.2018.01.001>
- Bott MHP (1960) The use of rapid digital computing methods for direct gravity interpretation of sedimentary basins. *Geophys J Int* 3(1): 63-67.
<https://doi.org/10.1111/j.1365-246X.1960.tb00065.x>
- Bozkurt E (2001) Neotectonics of Turkey - A synthesis. *Geodinamica Acta* 14: 3-30.
<https://doi.org/10.1080/09853111.2001.11432432>
- Bozkurt E, Mittwede SK (2001) Introduction to the geology of Turkey—a synthesis. *Int Geol Rev* 43(7): 578-594.
<https://doi.org/10.1080/00206810109465034>
- Bozkurt E (2003) Origin of NE- trending basins in western Turkey. *Geodin Acta* 61: 8.
[https://doi.org/10.1016/S0985-3111\(03\)00002-0](https://doi.org/10.1016/S0985-3111(03)00002-0)
- Bozkurt E, Sözbilir H (2004) Tectonic Evolution of the Gediz Graben: Field Evidence for an Episodic, Two-Stage Extension in Western Turkey. *Geol Mag* 141: 63-79.
<https://doi.org/10.1017/S0016756803008379>
- Bozkurt E, Mittwede SK (2005) Introduction: evolution of Neogene extensional tectonics of western Turkey. *Geodin Acta* 18: 153-165.
<https://doi.org/10.3166/ga.18.153-165>
- Brogi A, Capezzuoli E, Alçiçek MC, et al. (2014) Evolution of a fault-controlled travertine fissure-ridge in the western Anatolia extensional province: the Çukurbağ fissure-ridge (Pamukkale, Turkey). *J Geol Soc* 171: 425-441.
<https://doi.org/10.1144/jgs2013-034>
- Cambazoğlu S, Yala GP, Eker AM, et al. (2019) Geothermal resource assessment of the Gediz Graben utilizing TOPSIS Methodology. *Geothermics* 80: 92-102.
<https://doi.org/10.1016/j.geothermics.2019.01.005>
- Cooper GRJ, Cowan DR (2006) Enhancing potential field data using filters based on the local phase. *Comput Geosci* 32(10): 1585-1591.
<https://doi.org/10.1016/j.cageo.2006.02.016>
- Cooper GRJ, Cowan DR (2008) Edge enhancement of potential-field data using normalized statistics. *Geophysics* 73(3): 1-4.
<https://doi.org/10.1190/1.2837309>
- Cordell L (1973) Gravity analysis using an exponential density-depth function—San Jacinto Graben, California. *Geophysics* 38(4): 684-690.
<https://doi.org/10.1190/1.1440367>
- Cordell L (1979) Gravimetric expression of graben faulting in Santa Fe Country and the Espanola basin, New Mexico. In: Intersoll, R.V. (Ed.), *Guidebook to Santa Fe Country*, 30th Field Conference. New Mexico: Geological Society 59-64.
- Cordell L, Grauch VJS (1985) Mapping basement magnetization zones from aeromagnetic data in the San Juan basin, New Mexico. In: Hinze WJ (ed.) *The utility of regional gravity and magnetic anomaly maps*. *Soc Expl Geophys* pp 181-197
<https://doi.org/10.1190/1.0931830346.ch16>
- Cordell L, Henderson RG (1968) Iterative three-dimensional solution of gravity anomaly data using a digital computer. *Geophysics* 33: 596-601.
<https://doi.org/10.1190/1.1439955>
- Çakır Z (1999) Along-strike discontinuity of active normal faults and its influence on Quaternary travertine deposition; examples from western Turkey. *Turk J Earth Sci* 8(1): 67-80.
- Çiftçi NB, Bozkurt E (2009) Pattern of normal faulting in the Gediz Graben, SW Turkey. *Tectonophysics* 473(1-2): 234-260.
<https://doi.org/10.1016/j.tecto.2008.05.036>
- Çiftçi NB, Bozkurt E (2009) Evolution of the miocene sedimentary fill of the Gediz Graben, SW Turkey. *Sediment Geol* 216(3-4): 49-79.
<https://doi.org/10.1016/j.sedgeo.2009.01.004>
- Dewey JF, Şengör AC (1979) Aegean and surrounding regions: complex multiplate and continuum tectonics in a convergent zone. *Geol Soc Am Bull* 90(1): 84-92.
[https://doi.org/10.1130/0016-7606\(1979\)90<84:AASRCM>2.0.CO;2](https://doi.org/10.1130/0016-7606(1979)90<84:AASRCM>2.0.CO;2)
- Dilalos S, Alexopoulos JD, Lozios S (2019) New insights on subsurface geological and tectonic structure of the Athens basin (Greece), derived from urban gravity measurements. *J Appl Geophys* 167: 73-105.
<https://doi.org/10.1016/j.jappgeo.2019.04.024>
- Dilek Y, Whitney DL (2000) Cenozoic Crustal Evolution in Central Anatolia: Extension, Magmatism, and Landscape Development. In: Panayides, I., Xenophontos, C., Malpas, J., eds., *Proceedings of the Third International Conference on the Geology of the Eastern Mediterranean*: Geological Survey Department. Nicosia, Cyprus. pp 183-192.
- Du W, Wu Y, Guan Y, et al. (2017) Edge detection in potential field using the correlation coefficients between the average and standard deviation of vertical derivatives. *J Applied Geophys* 143: 231-238.
<https://doi.org/10.1016/j.jappgeo.2017.01.002>
- Emre Ö, Duman TY, Özalp S, et al. (2013) *The Annotated Active Fault Map of Turkey*. Scale 1: 1.250.000, General Directorate of Mineral Research and Exploration, Special Publication Series-30, Ankara-Turkey (In Turkish).

- <http://yerbilimleri.mta.gov.tr/home.aspx> (Accessed on 7 February 2022)
- Erdogan E, Candansayar ME (2017) The conductivity structure of the Gediz Graben geothermal area extracted from 2D and 3D magnetotelluric inversion: Synthetic and field data applications. *Geothermics* 65: 170-179.
<https://doi.org/10.1016/j.geothermics.2016.09.007>
- Eyidoğan H, Jackson JA (1985) A seismological study of normal faulting in the Demirci, Alaşehir and Gediz earthquake of 1960-1970 in western Turkey, implications for the nature and geometry of deformation in the continental crust. *Geophys J R Astron Soc* 81: 569-607.
<https://doi.org/10.1111/j.1365-246X.1985.tb06423.x>
- Ferreira FJ, de Souza J, Bongioio ABS, et al. (2013) Enhancement of the total horizontal gradient of magnetic anomalies using the tilt angle. *Geophysics* 78 (3): J33-J4.
<https://doi.org/10.1190/geo2011-0441.1>
- Frohlich C, Davis S (1993) Teleseismic b-values: or, much ado about 1.0. *J Geophys Res* 98: 631-644.
<https://doi.org/10.1029/92JB01891>
- Gessner K, Collins AS, Ring U, et al. (2004) Structural and thermal history of poly-orogenic basement: U-Pb geochronology of granitoid rocks in the southern Menderes Massif, Western Turkey. *J Geol Soc* 161:93-101
<https://doi.org/10.1144/0016-764902-166>
- Gessner K, Gallardo LA, Markwitz V, et al. (2013) What caused the denudation of the Menderes Massif: review of crustal evolution, lithosphere structure, and dynamic topography in southwest Turkey. *Gondwana Res* 24(1): 243-274.
<https://doi.org/10.1016/j.gr.2013.01.005>
- Göncüoğlu MC (2010) Introduction to the Geology of Turkey: Geodynamic evolution of the pre-Alpine and Alpine terranes. General Directorate of Mineral. Res. Explor., Monography Series No.5, pp 1-66.
- Granser H (1987) Three-dimensional interpretation of gravity data from sedimentary basins using an exponential density-depth function. *Geophys Prospect* 35: 1030-1041.
<https://doi.org/10.1111/j.1365-2478.1987.tb00858.x>
- Gutenberg B, Richter CF (1955) Magnitude and energy of earthquakes. *Nature* 176(4486): 795-795.
- Gürer A, Pine A, Gürer F, et al (2002) Resistivity distribution in the Gediz Graben and its implications for crustal structure. *Turk J Earth Sci* 11: 5-26.
- Hacıoğlu Ö, Başokur AT, Diner Ç, et al. (2020) The effect of active extensional tectonics on the structural controls and heat transport mechanism in the Menderes Massif geothermal province: Inferred from three-dimensional electrical resistivity structure of the Kurşunlu geothermal field (Gediz Graben, western Anatolia). *Geothermics* 85: 101708.
<https://doi.org/10.1016/j.geothermics.2019.07.006>
- Hakyemez Y, Göktaş F, Erkal T (2013) Gediz grabeninin Kuvaterner jeolojisi ve evrimi [Quaternary geology and evolution of the Gediz graben]. *Türkiye Jeoloji Bülteni* 56(2): 1-26.
- Hançer M (2013) Study of the structural evolution of the Babadag-Honaz and Pamukkale fault zones and the related earthquake risk potential of the Buldan region in SW Anatolia, East of the Mediterranean. *J Earth Sci* 24(3): 397-409.
<https://doi.org/10.1007/s12583-013-0333-2>
- Hetzel R, Romer RL, Candan O, et al (1998) Geology of the Bozdağ area, central Menderes Massif, SW Turkey: Pan-African basement and Alpine deformation. *Geol Rundsch* 87: 394-406.
<https://doi.org/10.1007/s005310050218>
- Irmak TS (2013) Focal mechanisms of small-moderate earthquakes in Denizli Graben (SW Turkey). *Earth Planet Sp* 65: 943-955
<https://doi.org/10.5047/eps.2013.05.011>
- İztan H, Yazman M (1990) Geology and hydrocarbon potential of the Alaşehir (Manisa) area, Western Turkey. *IESCA, Int Earth Sci Congr. on Aegean Regions*, 1-6 October, Proc. 1, İzmir. pp 327-338.
- Işık V, Seyitoğlu G, Çemen İ (2003) Ductile-brittle transition along the Alaşehir detachment fault and its structural relationship with the Simav detachment fault, Menderes Massif, western Turkey. *Tectonophysics* 374: 1-18.
[https://doi.org/10.1016/S0040-1951\(03\)00275-0](https://doi.org/10.1016/S0040-1951(03)00275-0)
- Jackson DD, Kagan YY (1999) Testable earthquake forecasts for 1999. *Seismol Res Lett* 70: 393-403.
<https://doi.org/10.1785/gssrl.70.4.393>
- Jolivet L, Faccenna C, Huet B, et al. (2013) Aegean tectonics: Strain localisation, slab tearing and trench retreat. *Tectonophysics* 597, 1-33.
<https://doi.org/10.1016/j.tecto.2012.06.011>
- Kalafat D (2016) Statistical Evaluation of Turkey Earthquake Data (1900-2015): A Case study. *EJJS* 2: 14-36.
- Kanthiya S, Mangkhemthong N, Morley CK (2019) Structural interpretation of Mae Suai Basin, Chiang Rai Province, based on gravity data analysis and modelling. *Heliyon* 5(2): e01232.
<https://doi.org/10.1016/j.heliyon.2019.e01232>
- Katsumata K (2006) Imaging the high b-value anomalies within the subducting Pacific plate in the Hokkaido corner. *EPS* 58: e49-e52.
<https://doi.org/10.1186/BF03352640>
- Kaymakçı N (2006) Kinematic development and paleostress analysis of the Denizli Basin (Western Turkey): Implications of spatial variation of relative paleostress magnitudes and orientations. *J Asian Earth Sci* 27: 207-222.
<https://doi.org/10.1016/j.jseae.2005.03.003>
- Kaypak B, Gökkaya G (2012) 3-D imaging of the upper crust beneath the Denizli geothermal region by local earthquake tomography, western Turkey. *J Volcanol Geotherm Res* 211-212: 47-60.
<https://doi.org/10.1016/j.jvolgeores.2011.10.006>
- Kebede H, Alemu A, Nedaw D (2021) Mapping geologic structures from Gravity and Digital Elevation Models in the Ziway-Shala Lakes basin; central Main Ethiopian rift. *Heliyon* 7(12): e08604.
<https://doi.org/10.1016/j.heliyon.2021.e08604>
- Khan PK (2005) Variation in dip-angle of the Indian plate subducting beneath the Burma plate and its tectonic implications. *Geosci Int J* 9:227-234.
<https://doi.org/10.1007/BF02910582>
- Koçyiğit A, Yusufoglu H, Bozkurt E (1999) Evidence from the Gediz Graben for episodic two-stage extension in western Turkey. *J Geol Soc London* 156: 605-616.
<https://doi.org/10.1144/gsjgs.156.3.0605>
- Koçyiğit A (2005) The Denizli Graben-Horst System and the eastern limit of western Anatolian continental extension: Basin fill, structure, deformational mode, throw amount and episodic evolutionary history, SW Turkey. *Geodin Acta* 18(3-4): 167-208.
<https://doi.org/10.3166/ga.18.167-208>
- Koçyiğit A, Devenci Ş (2007) A NS-trending active extensional structure, the Şuhut (Afyon) graben: commencement age of the extensional neotectonic period in the Isparta Angle, SW Turkey. *Turk J Earth Sci* 16(4): 391-416.
- Konak N, Şenel M (2002) Geological Map of Turkey in 1/500.000 Scale: Denizli Sheet. Ankara. Publication of Mineral Research and Exploration Directorate of Turkey (MTA).
- Le Pichon X, Angelier J (1979) The hellenic arc trench system: A key to the neotectonic evolution of the eastern Mediterranean area. *Tectonophysics* 60(1-2): 1-42.
[https://doi.org/10.1016/0040-1951\(79\)90131-8](https://doi.org/10.1016/0040-1951(79)90131-8)
- Le Pichon X, Angelier J (1981) The Aegean Sea. *Philosophical Transactions of Royal Society London* 300: 357-372. Ma, G.Q. 2013. Edge detection of potential field data using improved local phase filter. *Explor Geophys* 44(1): 36-41.
<https://doi.org/10.1098/rsta.1981.0069>
- Ma G, Li L (2012) Edge detection in potential fields with the normalized total horizontal derivative. *Comput Geosci* 41: 83-87.
<https://doi.org/10.1016/j.cageo.2011.08.016>

- McKenzie D (1972) Active tectonics of the Mediterranean region. *Geophys J Int* 30(2): 109-185.
<https://doi.org/10.1111/j.1365-246X.1972.tb02351.x>
- McKenzie DP (1978) Active tectonic of the mediterranean belt, aegean sea and surrounding regions. *Geophys J R Astr* 30(2): 109-185.
<https://doi.org/10.1111/j.1365-246X.1978.tb04759.x>
- Meng J, Sinoplu O, Zhou Z, et al. (2021) Greece and Turkey Shaken by African tectonic retreat. *Sci Rep* 11(1): 1-10.
<https://doi.org/10.1038/s41598-021-86063-y>
- Mercier JL, Sorel D, Vergely P, Simeakis K (1989) Extensional tectonic regimes in the Aegean basins during the Cenozoic. *Basin Res* 2(1): 49-71.
<https://doi.org/10.1111/j.1365-2117.1989.tb00026.x>
- Meulenkamp JE, Wortel WJR, Van Wamel WA et al. (1988) On the hellenic subduction zone and geodynamic evolution of Crete since the Late Middle Miocene. *Tectonophysics* 146(1-4): 203-215.
[https://doi.org/10.1016/0040-1951\(88\)90091-1](https://doi.org/10.1016/0040-1951(88)90091-1)
- Miller HG, Singh V (1994) Potential field tilt-a new concept for location of potential field sources. *J Appl Geophys* 32(2-3): 213-217.
[https://doi.org/10.1016/0926-9851\(94\)90022-1](https://doi.org/10.1016/0926-9851(94)90022-1)
- Mogi K (1962) Magnitude-frequency relation for elastic shocks accompanying fractures of various materials and some related problems in earthquakes. *Bull Earthquake Res Inst Univ Tokyo* 40: 831-853.
<https://doi.org/10.15083/0000033759>
- Öncel AO, Wilson T, Nishizawa O (2001) Size scaling relationships in the active fault networks of Japan and their correlation with Gutenberg-Richter b values. *J Geophys Res* 106: 827-841.
<https://doi.org/10.1029/2000JB900408>
- Öncel AO, Wilson TH (2002) Space-Time correlations of seismotectonic parameters and examples from Japan and Turkey preceding the İzmit Earthquake. *Bull Seismol Soc Am* 92: 339-350.
<https://doi.org/10.1785/0120000844>
- Özbakir AD, Govers R, Wortel R (2017) Active faults in the Anatolian-Aegean plate boundary region with Nubia. *Turk J Earth Sci* 26(1): 30-56.
<https://doi.org/10.3906/yer-1603-4>
- Öztürk S (2018) "Earthquake hazard potential in the Eastern Anatolian part of Turkey: seismotectonic b and Dc-values, and precursory quiescence Z-value," *Front Earth Sci* 12 (1) : 215-236.
<https://doi.org/10.1007/s11707-017-0642-3>
- Öztürk S, Gerdan S (2020) A general overview on the region-time behaviors of the recent earthquake activity in the Marmara region of Turkey. *Sigma J Eng Nat Sci* 38(3): 1623-1641.
- Paton S (1992) Active normal faulting, drainage patterns and sedimentation in SW Turkey. *J Geol Soc London* 149: 1031-1044.
<https://doi.org/10.1144/gsjgs.149.6.1031>
- Purvis M, Robertson A (2005) Sedimentation of the Neogene-Recent Alaşehir (Gediz) continental graben system used to test alternative tectonic models for western (Aegean) Turkey. *Sediment Geol* 173(1-4), 373-408.
<https://doi.org/10.1016/j.sedgeo.2003.08.005>
- Papazachos CB (1999) Seismological and GPS evidence for the Aegean-Anatolia interaction. *Geophys Res Lett* 26: 2653-2656.
<https://doi.org/10.1029/1999GL900411>
- Pham LT, Oksum E (2018) GCH_gravinv: A MATLAB-based program for inverting gravity anomalies over sedimentary basins. *Comput Geosci* 120: 40-47.
<https://doi.org/10.1016/j.cageo.2018.07.009>
- Polat O, Gok E, Yilmaz D (2008) Earthquake hazard of aegean extension region, Turkey: *Turk J Earth Sci* 17: 593-614.
- Polat G (2022) Spatial analysis of b-value variability in Elazığ city and the surrounding area (Eastern Turkey). *Acta Geophys* 70(1): 15-25.
- Poyraz F, Hastaoğlu KO, Koçbulut F, et al. (2019) Determination of the block movements in the eastern section of the Gediz Graben (Turkey) from GNSS measurements. *J Geodyn* 123: 38-48.
<https://doi.org/10.1016/j.jog.2018.11.001>
- Ramotoroko CD, Ranganai RT, Nyabeze P (2016) Extension of the Archaean Madibe-Kraaipan granite-greenstone terrane in southeast Botswana: Constraints from gravity and magnetic data. *J African Earth Sci* 123: 39-56.
<https://doi.org/10.1016/j.jafrearsci.2016.06.016>
- Reasenberg P (1985) Second-order moment of central California seismicity, 1969-82. *J Geophys Res* 90: 5479-5495.
<https://doi.org/10.1029/JB090iB07p05479>
- Rezaie M, Moradzadeh A, Kalate AN, et al. (2017) 3D modelling of Trompsburg Complex (in South Africa) using 3D focusing inversion of gravity data. *J African Earth Sci* 130: 1-7.
<https://doi.org/10.1016/j.jafrearsci.2017.03.002>
- Sainz-Maza S, Montesinos FG, Martí J, et al. (2017) Structural interpretation of El Hierro (Canary Islands) rifts system from gravity inversion modelling. *Tectonophysics* 712: 72-81.
<https://doi.org/10.1016/j.tecto.2017.05.010>
- Sarı C, Şalk M (2006) Sediment thicknesses of the western Anatolia graben structures determined by 2D and 3D analysis using gravity data. *J Asian Earth Sci* 26: 39-48.
<https://doi.org/10.1016/j.jseaes.2004.09.011>
- Scholz CH (1968) The frequency-magnitude relation of microfracturing in rock and its relation to earthquakes, *Bull Seismol Soc Am* 58: 399-415.
<https://doi.org/10.1785/BSSA0580010399>
- Seward D. et al. (2009) Cenozoic tectonic evolution of Naxos Island through a multi-faceted approach of fission-track analysis. *Geol Soc Lond Special Publ* 321:179-196.
<https://doi.org/10.1144/SP321.9>
- Selim ESI (2016) The integration of gravity, magnetic and seismic data in delineating the sedimentary basins of northern Sinai and deducing their structural controls. *J Asian Earth Sci* 115, 345-367.
<https://doi.org/10.1016/j.jseaes.2015.10.012>
- Seyitoğlu G, Scott B (1991) Late Cenozoic crustal extension and basin formation in west Turkey. *Geol Mag* 128(2): 155-166.
<https://doi.org/10.1017/S0016756800018343>
- Seyitoğlu G, Scott BC (1992a) The age of the Büyük Menderes Graben (west Turkey) and its tectonic implications, *Geol Mag* 129: 239-242.
<https://doi.org/10.1017/S001675680000830X>
- Seyitoğlu G, Scott BC (1992b) Late Cenozoic volcanic evolution of the northeastern Aegean region, *J Volcanol Geotherm Res* 54: 157-176.
[https://doi.org/10.1016/0377-0273\(92\)90121-S](https://doi.org/10.1016/0377-0273(92)90121-S)
- Seyitoğlu G, Scott BC (1996) The cause of N-S extensional tectonics in western Turkey: Tectonic escape vs. Backarc spreading vs. Orogenic collapse. *J Geodyn* 22: 145-153.
[https://doi.org/10.1016/0264-3707\(96\)00004-X](https://doi.org/10.1016/0264-3707(96)00004-X)
- Seyitoğlu G, Çemen İ, Tekeli O (2000) Extensional folding in the Alaşehir Gediz graben, western Turkey. *J Geol Soc London* 157: 1097-1100.
[https://doi.org/10.1016/0264-3707\(96\)00004-X](https://doi.org/10.1016/0264-3707(96)00004-X)
- Sözbilir H (2001) Geometry of macroscopic structures with their relations to the extensional tectonics: field evidence from the Gediz detachment, western Turkey. *Turk J Earth Sci* 10: 51-67.
- Sözbilir H (2002) Geometry and origin of folding in the Neogene sediments of the Gediz graben, western Anatolia, Turkey, *Geodin Acta* 15: 277-288.
<https://doi.org/10.1080/09853111.2002.10510761>
- Şengör AMC (1979) The north Anatolian transform fault: its age, offset and tectonic significance. *J Geol Soc London* 136: 269-282.
<https://doi.org/10.1144/gsjgs.136.3.0269>
- Şengör AMC, Yılmaz Y (1981) Tethyan evolution of Turkey: a plate tectonic approach. *Tectonophysics* 75: 181-241.Şengör, A.M.C. 1979. Türkiye'nin Neotektoniği'nin Esasları. T. J. K. Yayını el Kitabı.

- [https://doi.org/10.1016/0040-1951\(81\)90275-4](https://doi.org/10.1016/0040-1951(81)90275-4)
Şengör AMC, Görür N, Şaroğlu F (1985) Strike-slip faulting and related basin formation in zones of tectonic escape: Turkey as a case study. In: Biddle KT, Christie-Blick N, eds., *Strike-Slip Deformation, Basin Formation and Sedimentation*. Soc Eco Paleo and Min Spec Publ 37: 227-264.
<https://doi.org/10.2110/pec.85.37.0211>
- Spakman W, Wortel MJR, Vlaar NJ (1988) The Hellenic subduction zone: Tomographic image and its geodynamic implications. *Geophys Res Lett* 15: 60-63.
<https://doi.org/10.1029/GL015i001p00060>
- Taymaz T, Eyidoğan H, Jackson J (1991). Source parameters of large earthquakes in the East Anatolian Fault Zone (Turkey). *Geophys J Int* 106(3), 537-550.
<https://doi.org/10.1111/j.1365-246X.1991.tb06328.x>
- Temiz H, Gürsoy H, Tatar O (1998) Kinematics of late Pliocene-Quaternary normal faulting in the southeastern end of the Gediz Graben, Western Anatolia, Turkey: *International Geology Review* 40: 638-646.
<https://doi.org/10.1080/00206819809465228>
- Ten Veen JH, Boulton SJ, Alçiçek MC (2009) From palaeotectonics to neotectonics in the Neotethys realm. The importance of kinematic decoupling and inherited structural grain in SW Anatolia (Turkey): *Tectonophysics* 473: 261-281.
<https://doi.org/10.1016/j.tecto.2008.09.030>
- Turcotte D (1986) A fractal model of crustal deformation. *Tectonophysics* 132: 261-239.
[https://doi.org/10.1016/0040-1951\(86\)90036-3](https://doi.org/10.1016/0040-1951(86)90036-3)
- Turgay I, Özgüler ME, Şahin H (1980) Denizli-Buldan-Pamukkale geothermic energy exploration resistivity study, Ankara..M.T.A Report No: 6958. (In Turkish)
- Utsu T (1965) A method for determining the value of "b" in a formula $\log n = a - bM$ showing the magnitude-frequency relation for earthquakes. *Geophys Bull Hokkaido Univ* 13: 99-103.
- Utsu T (1999) Representation and analysis of the earthquake size distribution: a historical review and some new approaches. In *Seismicity Patterns, Their Statistical Significance and Physical Meaning*. Birkhäuser, Basel. pp. 509-535
https://doi.org/10.1007/978-3-0348-8677-2_15
- Uwiduhaye JDA, Mizunaga H, Saibi H (2018) Geophysical investigation using gravity data in Kinigi geothermal field, northwest Rwanda. *J African Earth Sci* 139: 184-192.
<https://doi.org/10.1016/j.jafrearsci.2017.12.016>
- Yılmaz Y, Genç ŞC, Gürer F, et al. (2000) When did the Western Anatolian grabens begin to develop? *Tectonics and Magm*. in Turkey and the Sur. Area. London: The Geological Society Spec Pub 173: 353-384.
<https://doi.org/10.1144/GSL.SP.2000.173.01.17>
- Yılmaz M, Gelisli K (2003) Stratigraphic-structural interpretation and hydrocarbon potential of the Alaşehir Graben, western Turkey. *Petroleum Geoscience* 9(3), 277-282.
<https://doi.org/10.1144/1354-079302-539>
- Yuan B, Xie W, Liu G, Zhang C (2012) Gravity field and tectonic features of Block L2 in the Lamu basin, Kenya. *Geophys Pros* 60(1), 161-178.
<https://doi.org/10.1111/j.1365-2478.2011.00961.x>
- Yuan Y, Huang D, Yu Q, Lu P (2014) Edge detection of potential field data with improved structure tensor methods. *J Appl Geophys* 108: 35-42.
<https://doi.org/10.1016/j.jappgeo.2014.06.013>
- Verduzco B, Fairhead JD, Green CM, et al. (2004) New insights into magnetic derivatives for structural mapping. *The Lead Edge* 23(2): 116-119.
<https://doi.org/10.1190/1.1651454>
- Wang J, Meng XH, Guo LH, et al. (2014) A correlation-based approach for determining the threshold value of singular value decomposition filtering for potential field data denoising. *J Geophys Eng* 11(5): 055007.
<https://doi.org/10.1088/1742-2132/11/5/055007>
- Wang J, Meng X, Li F (2015) Improved curvature gravity gradient tensor with principal component analysis and its application in edge detection of gravity data. *J Appl Geophys* 118: 106-114. .
<https://doi.org/10.1016/j.jappgeo.2015.04.013>
- Wang J, Meng X, Li F (2017) New improvements for lineaments study of gravity data with improved Euler inversion and phase congruency of the field data. *J Appl Geophys* 136: 326-334.
<https://doi.org/10.1016/j.jappgeo.2016.11.017>
- Warren NW, Latham GV (1970) An experimental study of thermally induced microfracturing and its relation to volcanic seismicity. *J Geophys Res* 75(23): 4455-4464.
<https://doi.org/10.1029/JB075i023p04455>
- Wiemer S (2001) A software package to analyze seismicity: ZMAP. *Seismol Res Lett* 72: 373-382.
<https://doi.org/10.1785/gssrl.72.3.373>
- Wiemer S, Wyss M (2000) Minimum magnitude of completeness in earthquake catalogs: Examples from Alaska, the western United States, and Japan. *Bull Seismol Soc Am* 90(4): 859-869.
<https://doi.org/10.1785/0119990114>
- Westaway R (1990) Block rotation in western Turkey: 1. Observational evidence. *J Geophys Res Solid Earth* 95(B12): 19857-19884.
<https://doi.org/10.1029/JB095iB12p19857>
- Westaway R (1993) Neogene evolution of the Denizli region of western Turkey. *J Struct Geol* 15(1): 37-53.
[https://doi.org/10.1016/0191-8141\(93\)90077-N](https://doi.org/10.1016/0191-8141(93)90077-N)
- Westaway R, Guillou H, Yurtmen S, et al. (2005) Constraints on the timing and regional conditions at the start of the present phase of crustal extension in western Turkey, from observations in and around the Denizli region: *Geodin Acta* 18: 209-238.
<https://doi.org/10.3166/ga.18.209-238>
- Wijns C, Perez C, Kowalczyk P (2005) Theta map: edge detection in magnetic data. *Geophysics* 70(4): L39-L43.
<https://doi.org/10.1190/1.1988184>
- Wilson T, Kato H (1992) Interpretation of the Matsumoto Basin gravity low. 31-41.
- Wilson T, Kato H (1995) Gravity Model Studies of the Northern Fossa Magna: Central Honshu, Japan. *Bull Geolog Survey Japan* 46: 1-22.
- Wyss M, Matsumura S (2002) Most likely locations of large earthquakes in the Kanto and Tokai areas, Japan, based on the local recurrence times. *Phys Earth Planet Inter* 131(2): 173-184.
[https://doi.org/10.1016/S0031-9201\(02\)00036-5](https://doi.org/10.1016/S0031-9201(02)00036-5)
- Zhou W, Du X, Li J (2013) The limitation of curvature gravity gradient tensor for edge detection and a method for overcoming it. *J Appl Geophys* 98: 237-242.
<https://doi.org/10.1016/j.jappgeo.2013.09.008>